

New mechanistic insight into the non-heme dioxygenase AsqJ-catalyzed epoxidation reaction

Hsuan-Jen Liao (廖宣任)¹, **Wei-Chen Chang**², **Nei-Li Chan** (詹迺立)¹

¹ *Institute of Biochemistry and Molecular Biology, College of Medicine, National Taiwan University, Taipei, Taiwan*

² *Department of Chemistry, North Carolina State University, Raleigh, U.S.*

nlchan@ntu.edu.tw

Abstract

AsqJ, a non-heme Fe^{II}/2-oxoglutarate-dependent dioxygenase recently discovered in *Aspergillus nidulans*, catalyzes the sequential desaturation and epoxidation of the substrate cyclopeptin to produce cyclophenin. These two AsqJ-mediated oxidation steps require the O₂-induced breakdown of 2-oxoglutarate into succinate and CO₂, which drives the formation of a high-valent ferryl-oxo (Fe^{IV}-oxo) species as an oxidative intermediate. Crystal structures of the AsqJ in its Ni^{II}-bound state and in complexes with cyclopeptin and its analogs have already been determined. However, a more complete and detailed mechanistic picture of the AsqJ-mediated reactions has remained unexplored. Here, we report three high-resolution crystal structures of AsqJ in its substrate (dehydrocyclopeptin)-bound, intermediate and product (cyclophenin)-bound complexes during AsqJ-catalyzed epoxidation. The substrate-bound AsqJ structure provides the first visualization of iron-coordinated O₂ in the 2OG-depednet dioxygenase superfamily. Moreover, an intermediate structure with continuous electron density being observed between the oxo group and C10 of dehydrocyclopeptin suggests the AsqJ-mediated epoxidation most likely starts from the O-C10 bond formation. We have also resolved for the first time the product-bound AsqJ complex, which is likely resulted from an in-crystal reaction. We have characterized two additional crystal structures of AsqJ in complex with a 2-CF₃-bound analog, which may explain why this analog is less reactive toward epoxidation. The mechanistic implications of these observations will be presented during the meeting.

Keywords – *O-C10 bond, carbocation, epoxidation*

Introduction

AsqJ, an iron(II) and 2-oxoglutarate (Fe/2OG) enzyme, has recently been discovered in viridicatin-type alkaloid biosynthesis in *Aspergillus nidulans*. It catalyzes two consecutive reactions: a C=C bond formation and an epoxidation to enable formation of the 6,6-bicyclic core of the viridicatin scaffold. However, mechanistic understanding of AsqJ-catalyzed desaturation has not been obtained.

Epoxide (oxirane) functional group is widely distributed in numerous natural products, which display a broad spectrum of biological activities, including antibacterial, antifungal, antiviral, and antitumor activities. In nature, two strategies are utilized to install epoxide, namely a formal dehydrogenation by cleaving a C-H and an O-H bond on two adjacent carbons, and an oxygen atom insertion (oxygen atom transfer, OAT) reaction onto an olefin moiety of the substrate (Scheme 1). In most cases, the epoxidation is initiated by highly reactive intermediates that are derived from different cofactors, such as flavin, thiolate-heme, non-heme di-iron, or non-heme mononuclear iron. For non-heme mononuclear iron enzymes, epoxidation through the dehydrogenation strategy has been reported in the biosyntheses of scopolamine by hyoscyamine 6 β -hydroxylase (H6H), of fosfomycin by 2-hydroxyl propyl

phosphonate epoxidase (HppE), of clavulanic acid by clavamate synthase (CAS), and of loline by LolO. In the same time, epoxidation through oxygen atom addition is reported in the biosynthesis of N β -epoxy-succinamoyl-DAP-Val by DdaC, of pentalenolactone by PenD (PntD), and of quinolone alkaloid by the recently discovered AsqJ (Scheme 1). Mechanistic understandings of enzymatic epoxidation through the oxygen insertion onto an olefin moiety are mainly derived from the studies on thiolate-heme containing epoxidases, such as chloroperoxidases (CPOs) and cytochrome P450s. Briefly, the C-O bonds of an epoxide can be installed in a concerted fashion or a stepwise manner via a discrete radical or cation intermediate. Here in, we use AsqJ as an example to reveal non-heme iron enzyme catalyzed epoxidation by using a multi-faceted approach. This approach utilizes LC-MS analysis, pre-steady state kinetics probed by stopped-flow optical absorption, spectroscopic characterizations using Mössbauer and electron paramagnetic resonance (EPR), X-ray crystallography, and density functional theory calculations to derive detailed molecular level understandings on the AsqJ reactivity. Along with its native substrate (2-OMe), several para-substituted analogs (2-H, 2-F and 2-CF₃) with varying electron donating/withdrawing ability are

used in this study to reveal reactivity trend in AsqJ catalyzed epoxidation.

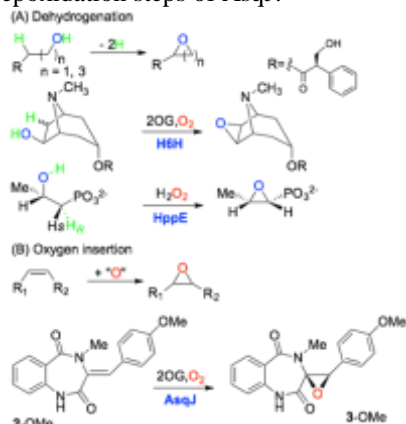
Results and Discussion

To provide structural insights into the AsqJ-catalyzed epoxidation, we have determined the crystal structures of AsqJ at different stages of the catalytic cycle. We first replaced **1-H** and acetate bound in the substrate and co-substrate binding site (ref), respectively, with **2-H** and 2OG by post-crystallization soaking. The resultant electron density map showed unambiguously the presence of **2-H** and 2OG (Figure. 1A), indicating that our ligand-exchange strategy was successful. In addition, a piece of electron density with one end connecting to the iron and features corresponding to O_2 was observed. Thus, it appears that we have obtained the crystal structure of the $AsqJ \cdot Fe \cdot 2OG \cdot 2-H \cdot O_2$ quinary complex. To our knowledge, this structure represents the first crystallographic visualization of an O_2 -bound state for a Fe/2OG enzyme family member. The refined Fe- O_2 bond length is 2.4 Å and the Fe-O1-O2 bond angle is 113°. As expected, the Fe-coordinated O_2 is located in trans with respect to H134 and is spatially close to the bidentate α -keto acid moiety of 2OG, suitable for engaging in oxidative decarboxylation of 2OG and formation of the ferryl-oxo intermediate. The distances from the uncoordinated O_2 to C1 and C2 of 2OG are 2.67 Å and 2.66 Å, respectively.

When the post-crystallization ligand-exchange was performed in the presence of 0.5 mM ascorbate, interestingly, difference electron density peaks appeared around the bound **1-H**, 2OG, and O_2 , suggesting that chemical reaction may have taken place in the crystal under this condition. Reinterpretation of the electron density maps observed in the active site showed that 2OG and **1-H** had been converted to succinate and **2-H**, respectively, and that O_2 had been activated and rearranged, with an oxygen pointing at **2-H** (Figure 1B). Unexpectedly, a continuous electron density was observed between the oxo group and C10 of **2-H**, suggesting that the oxo group may become covalently linked to the C10. The speculated O-C10 bond formation is accompanied by a shift of oxo group from the expected axial position, causing $Nc-Fe-O$ angle to deviate from 180° by ~15°. The refined bond lengths of Fe-O and O-C10 are 2.1 and 2.0 Å, respectively. This structure implicates that the epoxidation of **2-H** is likely initiated by the oxygenation of C10, unlike an earlier speculation that the reaction starts from the attack on C3. It has been proposed that the formation of a hexa-coordinated ferryl-oxo intermediate with the oxo group trans to H211 is the prerequisite for AsqJ-catalyzed epoxidation. However, the Fe center of this structure is penta-coordinated with a distorted trigonal bipyramidal geometry, raising the possibility that water engagement may not be essential for this reaction.

Consistent with the occurrence of in-crystal epoxidation, the electron density maps derived from a **1-H**-bound crystal exposed to excess amount of 2OG and 1.0 mM ascorbate revealed the presence of **3-H**, 2OG and O_2 in

the active site (Figure 5C). This structure represents a product-bound, $AsqJ \cdot Fe \cdot 2OG \cdot 3-H \cdot O_2$ quinary complex. The presence of 2OG instead of succinate in the active site indicates that AsqJ binds 2OG with higher affinity. The refined Fe- O_2 bond length is 2.32 Å and the Fe-O1-O2 bond angle is 88° (Figure 1C). Collectively, these structures provide new information for the epoxidation steps of AsqJ.



Scheme 1. Examples of epoxidation catalyzed by non-heme iron enzymes via (A) dehydrogenation and (B) oxygen insertion.

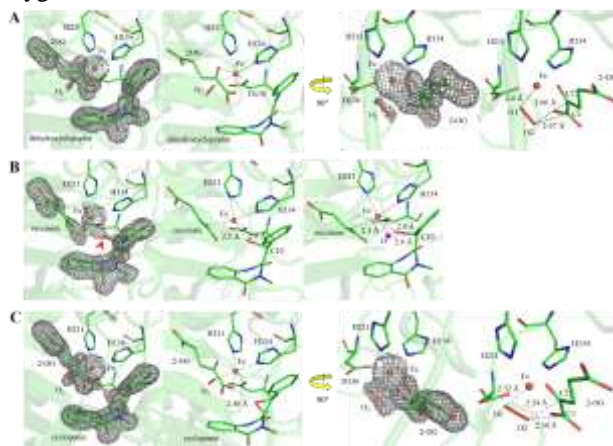


Figure 1. Crystallographic snapshots of AsqJ-catalyzed epoxidation. (A) The $AsqJ \cdot Fe \cdot 2OG \cdot 2-H \cdot O_2$ quinary complex. This structure may represent a state in which the substrate, 2OG, and O_2 are in place for initiating the epoxidation reaction. (B) An intermediate structure show that the AsqJ-catalyzed epoxidation may start from the oxygenation of C10. The red arrowhead points to the position of the oxo group. The magenta sphere (right panel) shows the modeled oxo group in an idealized axial position. (C) The product-bound $AsqJ \cdot Fe \cdot 2OG \cdot 3-H \cdot O_2$ quinary complex. The *2Fo-Fc* electron density maps are shown in grey mesh and contoured at 1.0 σ . The bound ligands (cofactors and substrates) and O_2 are shown in stick form. The Fe is shown as orange sphere. The carbon atoms of ligands and selected amino acid side chains are colored green. The remaining atoms are colored according to the CPK scheme.

Reference

H.-J. Liao, J. Li, J.-L. Huang, M. Davidson, I. Kurnikov, T.-S. Lin, J. L. Lee, M. Kurnikova, Y. Guo, N.-L. Chan and W.-c. Chang. *Angew Chem Int Ed Engl.*, 2018.